PROCEEDINGS OF SCIENCE

Perturbatively confined phase of QCD under imaginary rotation

Shi Chen,[a] **Kenji Fukushima**[b] **and Yusuke Shimada**[b,*]

[a] *School of Physics and Astronomy, University of Minnesota, Minneapolis, MN, 55455, USA*

[b] *Department of Physics, The University of Tokyo, 7-3-1 Hongo,Bunkyo-ku, Tokyo, 113-0033, Japan*

E-mail: s.chern.phys@gmail.com, fuku@nt.phys.s.u-tokyo.ac.jp, yshimada@nt.phys.s.u-tokyo.ac.jp

We perturbatively calculate the Polyakov loop potential at high temperature with imaginary angular velocity. Under the rapid imaginary rotation, the potential favors zero Polyakov loop, i.e., confinement. Moreover, this perturbatively confined phase can be smoothly connected to the hadronic phase. The potential calculation exhibits an inhomogeneous distribution of the Polyakov loop. There should appear a spatial interface separating the confined phase and the deconfined phase in imaginary rotating systems. We also evaluate the quark contribution to the Polyakov loop potential and confirm that spontaneous chiral symmetry breaking occurs in the perturbatively confined phase.

The XVIth Quark Confinement and the Hadron Spectrum Conference (QCHSC24)
19-24 August, 2024
Cairns Convention Centre, Cairns, Queensland, Australia

*Speaker

 ISSN 1824-8039 . Published by SISSA Medialab.

PoS(QCHSC24)151

1. Introduction

Confinement and chiral symmetry breaking are long-standing problems in Quantum Chromodynamics (QCD). One way to understand these phenomena is to research the properties of QCD matter under several environments. At finite temperatures, pure gluonic systems (or systems with infinitely heavy quarks) have the center symmetry, which classifies confinement and deconfinement of gluons. If the quark mass is finite, then the center symmetry is explicitly broken and the (dis)order parameter of the center symmetry, i.e., the Polyakov loop becomes only an approximate measure of confinement. In the quark massless limit, chiral symmetry is exact and the chiral condensate classifies the chiral symmetry intact or broken phase. Various phases of QCD have been considered using these order parameters as a function of external environmental parameters. A known example is the quark chemical potential μ for a dense system.

In particular, the angular velocity ω has been attracting experimental and theoretical interests. As a remarkable experimental result, a substantial angular velocity $\omega \sim 10^{22}$ s^{-1} was reported in the heavy-ion collision [1]. The effects of rotation are theoretically similar to the effects of density or chemical potential [2–5]. Interestingly, rotation directly affects gluons and the angular velocity is a useful probe for confinement and deconfinement.

Chiral phase transition in rotating systems was considered by using the NJL model [3, 6]. For the confinement-deconfinement critical temperature, the hadron resonance gas model and holographic QCD model were used [7–11]. They obtained decreasing critical temperature. This is a natural result because a rotating system is similar to a system with finite density or the chemical potential, where the critical temperature is decreasing function for the chemical potential. However, the numerical results from lattice-QCD simulations [12–14] obtained opposite results. They considered imaginary angular velocity $\omega = i\Omega_{\rm I}$ since real rotation causes the sign problem as real chemical potential, and their $T_c(\Omega_{\rm I})$ is a quadratic decreasing function so they concluded that the critical temperature increases in real rotating systems. New other researches have been carried out and results with improved models supporting the lattice calculations have been obtained.

In this proceeding, we report the results of our two papers [15, 16]. We utilize the perturbative Polyakov loop potential to investigate rotation effects based on the first-principles approach. If the temperature is sufficiently high, QCD or the pure gluonic theory can be perturbatively analyzed due to the asymptotic freedom. Without rotation, our calculation is the same as obtaining the Gross–Pisarski–Yaffe–Weiss (GPY–W) potential [17–21]. We should also remark that our study is for *imaginary* rotating systems. Interestingly, systems with imaginary angular velocity contain rich physics. Our work discovered that imaginary rotating systems have a confined phase at any high temperature, that is, *perturbatively confined phase*.

2. Derivation of the Polyakov Loop Potential for Imaginary Rotating Systems

We shall perform the one-loop calculation to find the Polyakov loop potential which is known as GPY–W potential. To simplify the calculation, we adopt the following background method:

$$A_\mu = A_{{\rm B}\,\mu} + \mathcal{A}_\mu \,, \tag{1}$$

where we decompose the gauge field into two parts. The first term in the right line means the tree-level of the gauge field, which we call the background part. The background gauge field physically

corresponds to the classic solution of the action and the tree level calculation gives the result at high temperature limit. The second term corresponds to the dynamical gauge field and the effective potential is calculated up to the leading order of this dynamical gauge field. If the temperature is sufficiently high, the coupling constant is so small that the character of such systems can be obtained in this one-loop calculation.

At finite temperature, the fourth component of the gauge field A_τ can be diagonalized and represented by the Cartan subalgebra of $\mathfrak{su}(N)$. We shall describe the basis of the Cartan subalgebra as $\boldsymbol{H}$ and then we have

$$A_{\mathrm{B}\,\mu} = i\frac{\delta_{\mu,\tau}}{g\beta}\boldsymbol{\phi}\cdot\boldsymbol{H}\,, \tag{2}$$

with background parameters $\boldsymbol{\phi}$. The potential is written by these background parameters and minimized by optimizing the value of them. The favored values of the background parameters determine the character of the system because the Polyakov loop, the (dis)order parameter of the confinement-deconfinement phase transition is defined as

$$L = \frac{1}{N_\mathrm{c}}\,\mathrm{tr}\,\mathcal{P}\exp\left(ig\int_0^\beta A_\tau\,d\tau\right) \simeq \frac{1}{N_\mathrm{c}}\,\mathrm{tr}\,\exp\left(i\boldsymbol{\phi}\cdot\boldsymbol{H}\right). \tag{3}$$

Here the right hand is the leading order of the Polyakov loop. The system is confined if the Polyakov loop becomes zero. Since the background parameters and the Polyakov loop are closely related, our effective potential of the background parameters is also called the Polyakov loop potential. Or, one can rewrite the potential by using the Polyakov loop value.

To get the potential, we introduce the background covariant derivative by

$$D_{\mathrm{B}\,\mu} = \partial_\mu + igA_{\mathrm{B}\,\mu} = \partial_\mu + i\delta_{\mu,\tau}\,\beta^{-1}\boldsymbol{\phi}\cdot\boldsymbol{H}\,, \tag{4}$$

and the gauge fixing condition is as follows

$$D_{\mathrm{B}\,\mu}A^\mu = 0\,. \tag{5}$$

In this condition, the Yang–Mills gauge action becomes

$$\mathrm{tr}\;F_{\mu\nu}F^{\mu\nu} = \mathrm{tr}\,\left[F_{\mathrm{B}\,\mu\nu}F_\mathrm{B}^{\mu\nu} + 4F_{\mathrm{B}\,\mu\nu}D_\mathrm{B}^\mu\mathcal{A}^\nu + 2\mathcal{A}_\mu\left(-D_{\mathrm{B}\,\nu}D_\mathrm{B}^\nu\right)\mathcal{A}^\mu\right] + O(\mathcal{A}^3)\,, \tag{6}$$

which means that the partition function is obtained by the determinant of $-D_\mathrm{B}^2$ Laplacian. The partition function also has the ghost part, or the Fadev–Popov determinant, which is also obtained by the determinant of the Laplacian. Half of the gauge contribution, which corresponds to the non-physical modes of gluons, is canceled by them.

When one considers a rotating system, rotation effects should be included. Here we show a simple way to consider the rotation. In a rotating system, matter of course rotates in a static coordinate. However, when the coordinate also rotates, rotating matter becomes static. Then the above argument can be applied, except that the system has a non-trivial metric. When one fixes the z-axis as the rotation axis and adopts the cylindrical coordinate (r,θ,z,τ), the metric of such a space-time is represented as

$$g_{\mu\nu} = \begin{pmatrix} 1 & 0 & 0 & 0 \\ 0 & r^2 & 0 & r^2\Omega_\mathrm{I} \\ 0 & 0 & 1 & 0 \\ 0 & r^2\Omega_\mathrm{I} & 0 & 1+r^2\Omega_\mathrm{I}^2 \end{pmatrix}. \tag{7}$$

Here the case with pure imaginary angular velocity $\omega = i\Omega_{\rm I}$ is considered. The partition function is obtained from the Laplacian by taking the contraction in this metric. The effect of the curved space-time appears as the emergence of a new term containing the Christoffel symbol. This means we now have different results for gluons and ghosts, or we have different Laplacians for them. For the latter, the Laplacian of scalars, which we refer to as the scalar Laplacian, becomes

$$-G^2_{\rm B\,s} = -g^{\mu\nu}\left[D_{{\rm B}\,\mu}D_{{\rm B}\,\nu} - \Gamma^\lambda_{\mu\nu}D_{{\rm B}\,\lambda}\right] = -(D_{{\rm B}\,\tau} - \Omega_{\rm I}\partial_\theta)^2 - r^{-1}\partial_r(r\partial_r) - r^{-2}\partial_\theta^2 - \partial_z^2\,, \tag{8}$$

and for the former, the Laplacian of vectors becomes (using the scalar Laplacian)

$$\left(-G^2_{\rm B\,v}\right)_\mu{}^\nu = \begin{pmatrix} -G^2_{\rm B\,s} + r^{-2} & 2r^{-3}\,\partial_\theta & 0 & 0 \\ -2r^{-1}\,\partial_\theta & -r\,G^2_{\rm B\,s}\,r^{-1} + r^{-2} & 0 & 0 \\ 0 & 0 & -G^2_{\rm B\,s} & 0 \\ -2\Omega_{\rm I} r^{-1}\,\partial_\theta & 2\Omega_{\rm I} r^{-1}\,\partial_r & 0 & -G^2_{\rm B\,s} \end{pmatrix}. \tag{9}$$

The eigenvalues and eigenfunctions of these operators are needed to get the Polyakov loop potential. Here we skip the detailed derivation of the spectra but the result is as follows. The eigenfunction of the scalar Laplacian is

$$\Phi_{n,l,\boldsymbol{k},\boldsymbol{\alpha}}(x) = \frac{E_{\boldsymbol{\alpha}}}{\sqrt{2\pi\beta}}\, e^{i\left(\frac{2\pi n}{\beta}\tau + l\theta + k_z z\right)} J_l(k_\perp r)\,, \tag{10}$$

where $n, l \in \mathbb{Z}$, $\boldsymbol{k} := (k_\perp, k_z) \in \mathbb{R}^+\times\mathbb{R}$ and $\boldsymbol{\alpha}$ is an element of the set of roots Φ of $\mathfrak{su}(N)$. $E_{\boldsymbol{\alpha}}$ is an eigenmatrix for the Cartan matrix $\boldsymbol{H}$ corresponding to a root $\boldsymbol{\alpha}$: $D_{{\rm B}\,\tau}E_{\boldsymbol{\alpha}} = \left(\partial_\tau + i\beta^{-1}\boldsymbol{\phi}\cdot\boldsymbol{\alpha}\right)E_{\boldsymbol{\alpha}}$. J_l is the l-th order Bessel function. The corresponding eigenvalues are given by

$$\lambda_{n,l,\boldsymbol{k},\boldsymbol{\alpha}} = \left(\frac{2\pi n + \boldsymbol{\phi}\cdot\boldsymbol{\alpha}}{\beta} + l\Omega_{\rm I}\right)^2 + |\boldsymbol{k}|^2\,. \tag{11}$$

For the vector Laplacian, we have the same eigenvalues but four different eigenfunctions. Two of them are almost the same as scalar ones. They can be written as $\Xi^{(i)}_{n,l,\boldsymbol{k},\boldsymbol{\alpha}}(x) = \Phi_{n,l,\boldsymbol{k},\boldsymbol{\alpha}}(x)\,\xi^{(i)}$, where $\xi^{(1)} := (0,0,1,0)^T$ and $\xi^{(2)} := (0,0,0,1)^T$. The remaining two modes are

$$\Xi^{(\pm)}_{n,l,\boldsymbol{k},\boldsymbol{\alpha}}(x) = \frac{E_{\boldsymbol{\alpha}}\,\xi^{(\pm)}}{2\sqrt{\pi\beta}}\, e^{i\left(\frac{2\pi n}{\beta}\tau + l\theta + k_z z\right)} J_{l\pm1}(k_\perp r)\,, \tag{12}$$

where $\xi^{(\pm)} := (\pm i, r, 0, \Omega_{\rm I} r)^T$.

One should note that the first two modes and the remaining two modes have different indices for the Bessel function. The meaning becomes clear when one considers the meaning of l. From the eigenfunctions, this l is coupled with the angular velocity. That is, l refers to the total angular momentum. The Bessel function comes from our cylindrical coordinate formalism so that the indices correspond to the orbital angular momentum. The latter two modes then have ±1 spin angular momentum. They are the physical modes of gluons. In a later section, we see the case of fermions and we have $\pm1/2$ spin modes in their eigenfunctions.

The Polyakov loop potential is given from the spatial integrand of the free energy $F = -\beta^{-1}\left[\log\mathrm{Det}\left(-\mathrm{G}^2_{\rm B\,s}\right) - \frac{1}{2}\log\mathrm{Det}\left(-\mathrm{G}^2_{\rm B\,v}\right)\right]$ and it becomes

$$V_g(\boldsymbol{\phi};\tilde{\Omega}_{\rm I}) = \frac{1}{4\pi^2\beta}\sum_{\boldsymbol{\alpha}\in\Phi}\sum_{l\in\mathbb{Z}}\int_0^\infty k_\perp\,\mathrm{d}k_\perp \int_{-\infty}^\infty \mathrm{d}k_z\left[J^2_{l-1}(k_\perp r) + J^2_{l+1}(k_\perp r)\right] \times \mathrm{Re}\log\left[1 - e^{-\beta\sqrt{k_\perp^2+k_z^2} - il\beta\Omega_{\rm I} + i\boldsymbol{\phi}\cdot\boldsymbol{\alpha}}\right]. \tag{13}$$

Or, when the logarithm is expanded (and further calculation including the momentum integration is applied) we have an analytical form of the potential

$$V_g = -\frac{2T^4}{\pi^2}\sum_{\alpha\in\Phi}\sum_{l=1}^{\infty}\frac{\cos(l\boldsymbol{\phi}\cdot\boldsymbol{\alpha})\cos\left(l\tilde{\Omega}_{\mathrm{I}}\right)}{\left\{l^2+2\tilde{r}^2\left[1-\cos\left(l\tilde{\Omega}_{\mathrm{I}}\right)\right]\right\}^2}\,. \tag{14}$$

Here $\tilde{r} = rT$ and $\tilde{\Omega}_{\mathrm{I}} = \Omega_{\mathrm{I}}/T$ are the dimensionless parameter.

Naturally, when $\Omega_{\mathrm{I}} = 0$ is assigned, the potential reproduces the free energy of the free gluon gass or well-known GPY–W potential. The potential takes the minima at $\phi \in 2\pi\mathbb{Z}$, for example in $SU(2)$ case, which all gives ± 1 Polyakov loop value and so the system is always deconfined. Since our calculation method is for a high temperature system, this means that pure gluonic systems are deconfined at high temperatures. Our new results are for rotating systems with $\Omega_{\mathrm{I}} \neq 0$.

3. Perturbative Confinement at the Rotating Center

We shall consider the $r = 0$ case first. Here the argument of the Bessel function becomes zero and all terms with non-zero index vanish. In physics language, only s-wave appears when one sees the matter at the rotating center. The Polyakov loop potential is obtained by only the spin part and ± 1 spin angular momentum makes the term for gluons.

$$V_g(r=0) = \frac{1}{4\pi^2\beta}\sum_{\alpha\in\Phi}\sum_{l=\pm1}\int_0^\infty k_\perp\,\mathrm{d}k_\perp\int_{-\infty}^{\infty}\mathrm{d}k_z\,\mathrm{Re}\log\left[1-e^{-\beta\sqrt{k_\perp^2+k_z^2}-il\beta\Omega_{\mathrm{I}}+i\boldsymbol{\phi}\cdot\boldsymbol{\alpha}}\right]. \tag{15}$$

The momentum integration can be done numerically and the result for $SU(2)$ with different ϕ and $\tilde{\Omega}_{\mathrm{I}}$ values are shown in Fig. 1. As angular velocity increases, the shape of the potential curve flips and the minimum points move onto $\phi = \pi, 3\pi, \cdots$, where the corresponding Polyakov loop is zero. Therefore the high temperature systems are confined when imaginary rotation is imposed. A similar result is obtained for $SU(3)$. The right figure of Fig. 1 shows the evolution of the Polyakov loop value against the imaginary angular velocity for $SU(2)$ and $SU(3)$. The Polyakov loop vanishes as angular velocity increases and one observes the phase transition to the confined phase. This confined phase is a new confined phase at high temperature. We call this phase as *perturbatively confined phase* and this phenomenon as *perturbative confinement*.

One should note that the potential is 2π periodic for imaginary angular velocity as shown in the potential. This corresponds to the fact that gluon has one spin. The additional term to the partition function due to the rotation is given by the exponent of the coupling of the angular velocity and the angular momentum $\exp(\beta\,\boldsymbol{\omega}\cdot\boldsymbol{J})$. When the angular velocity is imaginary, provided the angular momentum corresponds to the angular derivative, this exponent leads to the angular shift $\exp\left(\tilde{\Omega}_{\mathrm{I}}\cdot l\partial_\theta\right)$ with total angular momentum l. For gluons, the total angular momentum is an integer, so an angular shift of 2π gives the same result. This is a 2π periodicity of imaginary angular velocity. From the derivation, this is a common property for imaginary rotating systems and the periodicity should appear regardless of the coordinate setting and the calculation method.

How does the perturbatively confined phase behave at low temperature? We know that the deconfined phase at high temperature changes into the Hadronic confined phase, but what happens to the high temperature confined phase? Here we give one suggestion to this question.

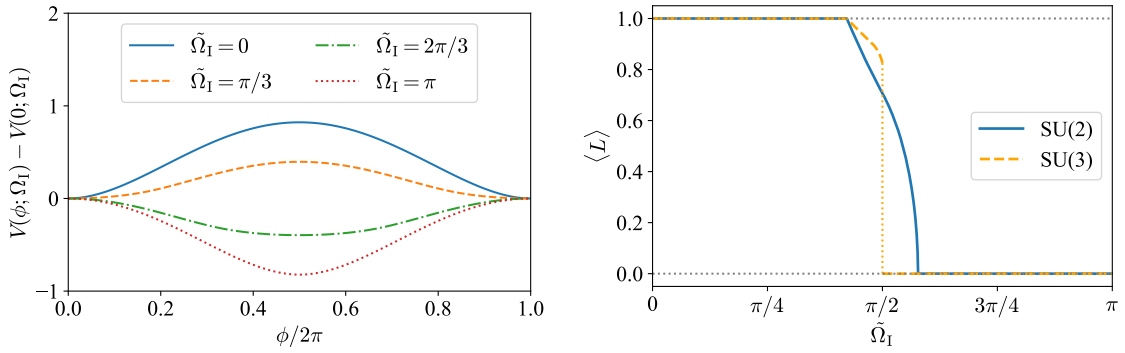

Figure 1: (Left) The values of the potential $V_g(r = 0)$ (made dimensionless with $1/T^4$ and to be zero at $\phi = 0$ by subtracting the offset) for $\tilde{\Omega}_I = 0, \pi/3, 2\pi/3, \pi$ in the color $SU(2)$ case. The graph is periodic in the direction of ϕ with a period of 2π. $\phi = \pi$ minimum point corresponds to confined systems. (Right) The expectation value of the Polyakov loop as a function of $\tilde{\Omega}_I$ for SU(2) (solid line) and SU(3) (dashed line) at $\tilde{r} = 0$. The system is confined if the Polyakov loop value vanishes. The graph is periodic in the direction of $\tilde{\Omega}_I$ with a period of 2π and symmetrical for $\tilde{\Omega}_I = 0$.

At low temperature, the ghost propagator is enhanced [22, 23]. Since ghosts cancel out the unphysical modes of gluons, or since the form of the ghosts' potential is inverted from the gluons' potential, such an enhancement causes an inversion of the potential. The minimum points of the potential shift, and the favored value of the Polyakov loop becomes zero. These ghosts' contribution to the confinement is the same in rotating systems. As discussed, the angular velocity couples with the total angular momentum. For ghosts, which have zero spin, the total angular momentum vanishes at the rotating center. Ghosts are therefore not affected by rotation. They always induce confinement regardless of the value of imaginary angular velocity.

As a result, the perturbatively confined phase become more confined when the temperature decrease. That is, systems with large angular velocities are always confined at any temperature. The perturbatively confined phase can be connected to the Hadronic phase without any phase transition. Our suggestion for the phase transition and the behavior of phase transition lines are illustrated in Fig. 2 as our phase diagram on $(\tilde{\Omega}_I, T)$ plane. Our calculation does not determine the critical temperature but it should increase since rapid rotation induces confinement. This expectation is consistent with some model calculations but discrepant with lattice calculations, and further analysis will be necessary to obtain a unified answer. Further studies may find another deconfined phase of imaginary rotating systems in the middle temperature region.

4. Spatial Phase Transition of Perturbatively Confined Phase

Previous studies have shown that the Polyakov loop value varies with distance from the rotating center and this leads to a spatial phase transition in rotating systems [24–26]. We also show this from our potential calculation with finite radius r and obtain the phase diagram on the distance and angular velocity plane. Here the terms with non-zero orbital angular momentum now come into the potential. The periodicity for the imaginary angular velocity is not changed but the shape and the minimum points of the potential can be drastically changed. This results in a change in the confinement-deconfinement behavior and the spatial phase transition of rotating systems.

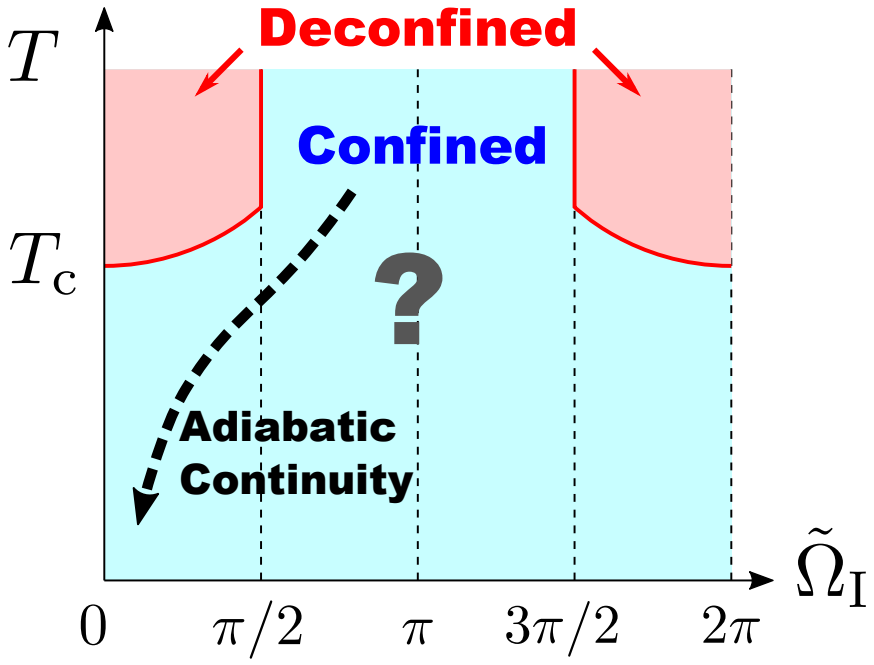

Figure 2: Conjectured phase diagram on $(\tilde{\Omega}_I, T)$ plane at the rotating center, $\tilde{r} = 0$, for the SU(3) case. The vertical first-order phase transition lines at high temperature are observed in our one-loop calculation. Increasing critical temperature and connectedness of the confined phases are suggested from our results. The diagram is 2π periodic for $\tilde{\Omega}_I$ direction.

As in the previous section, the Polyakov loop is calculated from the minimum point of the potential for a given fixed value of angular velocity and radius, and it is determined whether the system is confined or deconfined. The results are shown in Fig. 3. The left figure is for $SU(2)$ and the right figure is for $SU(3)$, with the Polyakov loop values indicated by the colors: the Polyakov loop is zero in the blue dense area (confined phase) and non-zero in orange and yellow area (deconfined phase). One can think of these figures as a phase diagram on $(\tilde{\Omega}_I, \tilde{r})$ plane of $SU(2)$ or $SU(3)$ pure gluonic system. The system is always deconfined when the angular velocity is small, while the confined phase appears when the angular velocity increases. In particular, even if the rotating center is confined, the system can be deconfined at a large radius away from the center. This implies the emergence of a spatial phase transition. Here we should emphasize that this $\tilde{r}$ dependence or inhomogeneity is qualitatively consistent with the lattice-QCD results [26]. They calculated the Polyakov loops at a temperature slightly below the critical temperature and found the same behavior: the value of the Polyakov loop increases as the distance from the center increases.

It is interesting that $SU(2)$ and $SU(3)$ have different behavior of the spatial phase transition. The latter especially has a different deconfined phase: the purple area in the right figure with $\tilde{\Omega}_I \sim \pi$ and $\tilde{r} \geq 0.5$, which have a Polyakov loop value of $1/3$ (in absolute value). Since the Polyakov loop value is 1 (in absolute value) in the ordinary deconfined phase, there may exist deconfined matter with unusual properties in this parameter region.

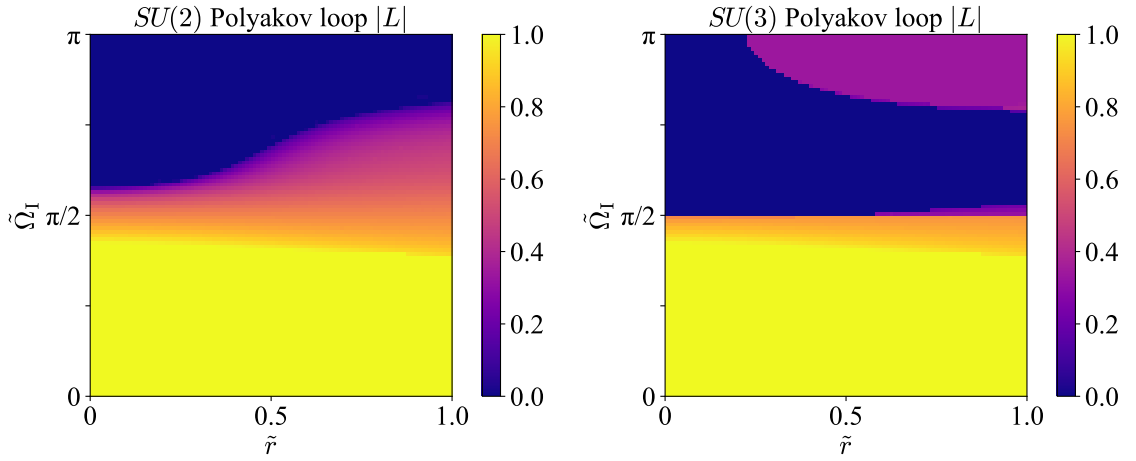

Figure 3: Map of the absolute value of the Polyakov loop at different fixed $(\tilde{\Omega}_{\rm I}, \tilde{r})$ for $SU(2)$ (Left) and $SU(3)$ (Right). Blue dense regions correspond to confined phases with zero Polyakov loop, while other regions correspond to deconfined phases with finite Polyakov loop. The boundary between the two regions represents the confinement-deconfinement phase transition line. A jump in the value of the Polyakov loop implies a first-order phase transition.

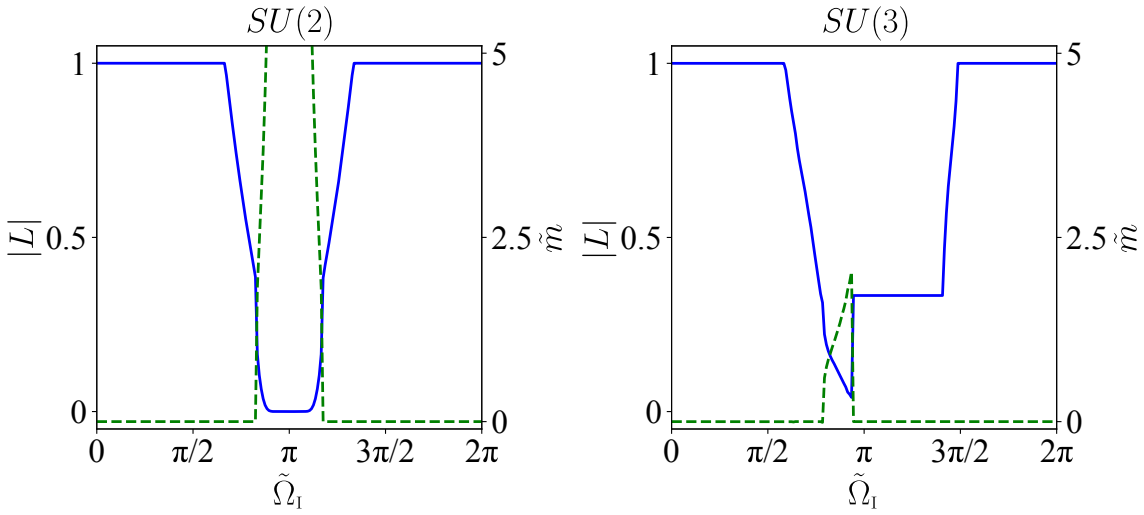

Figure 4: Polyakov loop $|L|$ (blue line) and dynamical mass $\tilde{m}$ (green dashed line) calculated from the minimum point of the potential at the rotating center $r = 0$ and different imaginary angular velocity $\tilde{\Omega}_{\rm I}$ for $N_c = 2$ (Left) or $N_c = 3$ (Right) and $N_f = 2$ QCD.

5. Chiral Symmetry Breaking in the Perturbatively Confined Phase

So far we have discussed pure gluonic systems. In this section, we extend our calculations to systems with massless quarks and discuss a rotating color $N_c = 2$ and flavor $N_f = 2$ QCD system. We shall take the cylindrical coordinate rotating with matter again, and the fermionic contribution to the partition function is the determinant of the Dirac operator in the rotating frame,

$$\mathcal{Z}_{\rm f} = {\rm Det}(\gamma^\mu {\rm G}_{{\rm B}\,\mu} + {\rm m})\,. \tag{16}$$

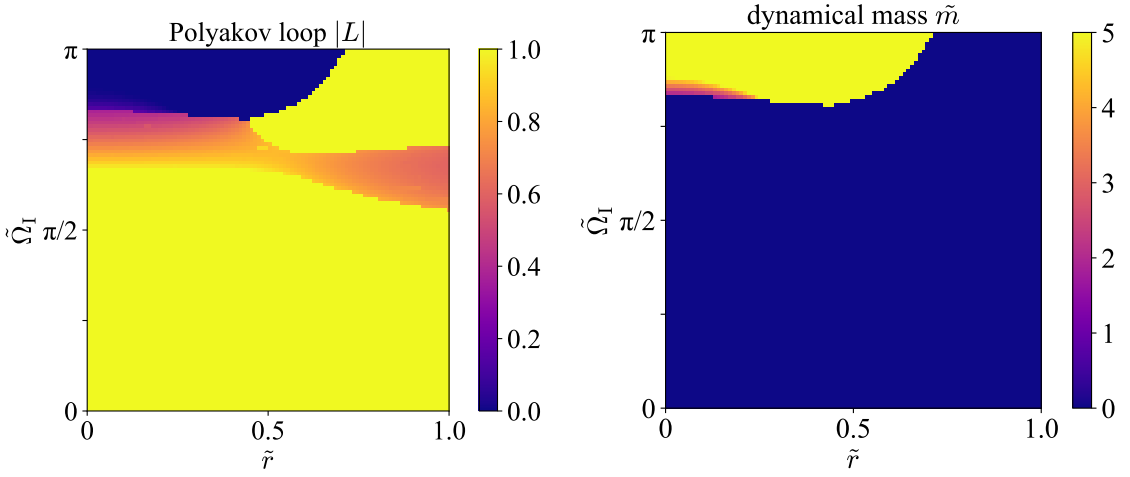

Figure 5: Map of the absolute value of the Polyakov loop (Left) and dynamical mass value (Right) at different fixed $(\tilde{\Omega}_{\rm I}, \tilde{r})$ for $N_c = N_f = 2$ QCD. Blue dense regions correspond to a confined phase with zero Polyakov loop (Left) or a chiral intact phase with zero chiral condensate (Right). The boundary between the blue dense region and regions with other colors represents the confinement-deconfinement or chiral symmetry breaking phase transition line. One can see that confined phase (zero Polyakov loop) and chiral broken phase (finite chiral condensate) appear on the same parameter region.

Here, $G_{{\rm B}\,\mu} = D_{{\rm B}\,\mu} - \Gamma_\mu$ is the covariant derivative including the $A_{{\rm B}\,\tau}$ background field with $\Gamma_\mu = -\frac{i}{4}\sigma^{ab}\,\omega_{\mu ab}$, where $\sigma^{ab} = \frac{i}{2}[\hat{\gamma}^a, \hat{\gamma}^b]$ and $\omega_{\mu ab} = g_{\rho\sigma}\, e_a^{\ \rho}\left(\partial_\mu e_b^{\ \sigma} + \Gamma^\sigma_{\mu\nu}\, e_b^{\ \nu}\right)$. We denote the gamma matrices of the flat space-time by $\hat{\gamma}^a$ and $\gamma^\mu = e_a^{\ \mu}\hat{\gamma}^a$. In our calculations, instead of using a model such as the Nambu—Jona-Lasinio model, we introduce the physical mass m of (anti-)quarks as a dynamical variable. The potential is a function of $\boldsymbol{\phi}$ and m, and the minimum point of the potential leads to the Polyakov loop and the quark dynamical mass (or chiral condensate).

The detailed calculation is omitted, but the result is as follows,

$$V_f(\boldsymbol{\phi}; \tilde{\Omega}_{\rm I}) = -\frac{1}{4\pi^2\beta}\sum_{\boldsymbol{\mu}\in\Phi_f}\sum_{l\in\mathbb{Z}}\int_0^\infty k_\perp\,{\rm d}k_\perp\int_{-\infty}^{\infty}{\rm d}k_z\left[J_l^2(k_\perp r) + J_{l+1}^2(k_\perp r)\right] \times {\rm Re}\log\left(1 + e^{i\left[\boldsymbol{\phi}\cdot\boldsymbol{\mu} - i\tilde{\Omega}_{\rm I}(l+1/2)\right] - \beta\sqrt{\boldsymbol{k}^2+m^2}}\right), \qquad (17)$$

where $\boldsymbol{\mu}$ is a fundamental weight of the $\mathfrak{su}(N)$ algebra and Φ_f denotes the set of the weights. The potential expression is similar to that of the gluon case, but this is for fermions so the logarithm has the opposite sign. Also, since the quark has $1/2$ spin, the total angular momentum which couples with angular velocity is half-integer. As a result, the fermionic potential is periodic for the angular velocity by 4π. This corresponds to the fact that fermions revert with a spatial 4π rotation (or angular shift) and fermions are anti-periodic in the imaginary time direction. This potential also leads to the well-known fermionic free gas potential by setting the angular velocity to zero.

The Polyakov loop and dynamical mass values at the potential minimum point are calculated at the rotating center and results are shown in Fig. 4. The graph has a 4π periodicity and is symmetric for $\tilde{\Omega}_{\rm I} = 0$. The development of the Polyakov loop is illustrated by the blue line and the dynamical mass is illustrated by the green line for $SU(2)$ (left) and $SU(3)$ (right) color QCD. If

the Polyakov loop is zero, then the system is confined and if the dynamical mass is finite, then the chiral symmetry is broken. As the angular velocity increases, the system becomes confined and the chiral symmetry is broken. Since the center symmetry is explicitly broken in systems containing fermions, the Polyakov loop is not strictly zero unless the dynamical mass diverges. In $SU(2)$, the favored dynamical mass diverges when $\tilde{\Omega}_{\rm I} \sim \pi$ and the Polyakov loop can be exactly zero. In $SU(3)$, the graph is slightly more complicated, but confinement and chiral symmetry breaking still occur almost simultaneously.

The same calculation can be done at finite distances away from the rotating center. Figure 5 shows the results of finding the minimum point of the potential with different $(\tilde{\Omega}_{\rm I}, \tilde{r})$ parameters. Here, we consider only the $N_c = N_f = 2$ QCD system. The potential has two variables ϕ and m, and the values of them at a potential minimum point correspond to the Polyakov loop and the chiral condensate. The map on the left plots the former and the map on the right plots the latter. The dark blue region corresponds to the zero value, which means a confined phase in the left map and a chiral intact phase in the right map. The boundary between the dark blue region and the other colors' region gives the phase transition line and a jump in values refers to a first-order phase transition. Our calculations show that a confined and chiral broken phase appears when $\tilde{\Omega}_{\rm I} \sim \pi$ and $\tilde{r}$ are small, and in particular we find that these two phases exist on the same parameter region. As in the pure gluonic system, a deconfined phase exists at large radii, and a spatial phase transition appears. A unique deconfined phase with an absolute value of the Polyakov loop not equal to 1 also appears here, which may indicate that the rotating QCD system contains a new and different deconfinement structure.

6. Conclusions

In this proceeding, we obtained the Polyakov loop potential by a one-loop perturbation calculation and clarified the properties of an imaginary rotating pure gluonic or QCD system at high temperature. As a result, we discovered a confined phase at high temperature (perturbatively confined phase), and it is suggested that this phase can be connected to the hadronic confinement phase at low temperature. Rotating systems are inhomogeneous: the perturbatively confined phase at the rotating center changes to a (possibly singular) deconfined phase at the finite radii. In addition, calculations with the dynamical quark mass revealed that the chiral symmetry is simultaneously broken in the perturbative confinement phase. Imaginary angular velocity is a novel theoretical device to tackle the mechanism of confinement and chiral symmetry breaking.

The consideration of imaginary rotating systems also allows us to explore the phenomena of real rotating systems that appear in high-energy experiments and neutron stars. However, one should be careful when extending them to real rotation systems. For example, if the potential is analytically continued to real rotation, the integral calculation becomes impossible due to the causality problem, so we need to impose a boundary condition on the system. The inhomogeneity of the rotating systems came from the emergence of the non-zero orbital angular momenta, and it is not surprising that such inhomogeneity appears in real rotation experiments as well.

Acknowledgments

This proceedings contribution is based on our published papers. The authors thank Maxim Chernodub, Yuki Fujimoto, Arata Yamamoto, and Xu-Guang Huang for useful discussions. They also thank Yuya Tanizaki for pointing out that the deconfined phase at low T is unlikely, which strengthens our speculation. Our works were supported by Japan Society for the Promotion of Science (JSPS) KAKENHI Grant No. 21J20877 (S.C.), 19K21874 (K.F.), 22H01216 (K.F.), Grant Nos. 22H01216 (K.F.) and 22H05118 (K.F.) and 21J20877 (S.C.) and JST SPRING, Grant Number JPMJSP2108 (Y.S.).

References

[1] STAR collaboration, *Global Λ hyperon polarization in nuclear collisions: evidence for the most vortical fluid*, *Nature* **548** (2017) 62 [1701.06657].

[2] H.-L. Chen, K. Fukushima, X.-G. Huang and K. Mameda, *Analogy between rotation and density for Dirac fermions in a magnetic field*, *Phys. Rev. D* **93** (2016) 104052 [1512.08974].

[3] X. Wang, M. Wei, Z. Li and M. Huang, *Quark matter under rotation in the NJL model with vector interaction*, *Phys. Rev. D* **99** (2019) 016018 [1808.01931].

[4] M.N. Chernodub and S. Gongyo, *Interacting fermions in rotation: chiral symmetry restoration, moment of inertia and thermodynamics*, *JHEP* **01** (2017) 136 [1611.02598].

[5] K. Fukushima, T. Shimazaki and L. Wang, *Mode decomposed chiral magnetic effect and rotating fermions*, *Phys. Rev. D* **102** (2020) 014045 [2004.05852].

[6] Y. Jiang and J. Liao, *Pairing Phase Transitions of Matter under Rotation*, *Phys. Rev. Lett.* **117** (2016) 192302 [1606.03808].

[7] Y. Fujimoto, K. Fukushima and Y. Hidaka, *Deconfining Phase Boundary of Rapidly Rotating Hot and Dense Matter and Analysis of Moment of Inertia*, *Phys. Lett. B* **816** (2021) 136184 [2101.09173].

[8] X. Chen, L. Zhang, D. Li, D. Hou and M. Huang, *Gluodynamics and deconfinement phase transition under rotation from holography*, *JHEP* **07** (2021) 132 [2010.14478].

[9] N.R.F. Braga, L.F. Faulhaber and O.C. Junqueira, *Confinement-deconfinement temperature for a rotating quark-gluon plasma*, *Phys. Rev. D* **105** (2022) 106003 [2201.05581].

[10] G. Yadav, *Deconfinement temperature of rotating QGP at intermediate coupling from M-theory*, *Phys. Lett. B* **841** (2023) 137925 [2203.11959].

[11] J.-H. Wang and S.-Q. Feng, *The rotation effect on the deconfinement phase transition in holographic QCD*, 2403.01814.

[12] V.V. Braguta, A.Y. Kotov, D.D. Kuznedelev and A.A. Roenko, *Study of the Confinement/Deconfinement Phase Transition in Rotating Lattice SU(3) Gluodynamics*, *Pisma Zh. Eksp. Teor. Fiz.* **112** (2020) 9.

[13] V.V. Braguta, A.Y. Kotov, D.D. Kuznedelev and A.A. Roenko, *Influence of relativistic rotation on the confinement-deconfinement transition in gluodynamics*, *Phys. Rev. D* **103** (2021) 094515 [2102.05084].

[14] J.-C. Yang and X.-G. Huang, *QCD on Rotating Lattice with Staggered Fermions*, 2307.05755.

[15] S. Chen, K. Fukushima and Y. Shimada, *Perturbative Confinement in Thermal Yang-Mills Theories Induced by Imaginary Angular Velocity*, *Phys. Rev. Lett.* **129** (2022) 242002 [2207.12665].

[16] S. Chen, K. Fukushima and Y. Shimada, *Inhomogeneous confinement and chiral symmetry breaking induced by imaginary angular velocity*, *Phys. Lett. B* **859** (2024) 139107 [2404.00965].

[17] D.J. Gross, R.D. Pisarski and L.G. Yaffe, *QCD and Instantons at Finite Temperature*, *Rev. Mod. Phys.* **53** (1981) 43.

[18] N. Weiss, *The Effective Potential for the Order Parameter of Gauge Theories at Finite Temperature*, *Phys. Rev. D* **24** (1981) 475.

[19] N. Weiss, *The Wilson Line in Finite Temperature Gauge Theories*, *Phys. Rev. D* **25** (1982) 2667.

[20] C.P. Korthals Altes, *Constrained effective potential in hot QCD*, *Nucl. Phys. B* **420** (1994) 637 [hep-th/9310195].

[21] A. Gocksch and R.D. Pisarski, *Partition function for the eigenvalues of the Wilson line*, *Nucl. Phys. B* **402** (1993) 657 [hep-ph/9302233].

[22] V.N. Gribov, *Quantization of Nonabelian Gauge Theories*, *Nucl. Phys. B* **139** (1978) 1.

[23] D. Zwanziger, *Fundamental modular region, Boltzmann factor and area law in lattice gauge theory*, *Nucl. Phys. B* **412** (1994) 657.

[24] M.N. Chernodub, *Inhomogeneous confining-deconfining phases in rotating plasmas*, *Phys. Rev. D* **103** (2021) 054027 [2012.04924].

[25] M.N. Chernodub, V.A. Goy and A.V. Molochkov, *Inhomogeneity of a rotating gluon plasma and the Tolman-Ehrenfest law in imaginary time: Lattice results for fast imaginary rotation*, *Phys. Rev. D* **107** (2023) 114502 [2209.15534].

[26] V.V. Braguta, M.N. Chernodub and A.A. Roenko, *New mixed inhomogeneous phase in vortical gluon plasma: first-principle results from rotating SU(3) lattice gauge theory*, 2312.13994.

PoS(QCHSC24)151